Consequences of Oil Spills on the Subsurface Resistivity of Soil in Biseni Community of Yenagoa Local Government Area of Bayelsa State in Niger Delta, Nigeria

***Adedokun, Isaac Oludayo., [2]Adetona, Abbass Adebayo**

[1]Department of Physics, Niger Delta University, Wilberforce Island, Bayelsa State, Nigeria

[2]Department of Physics, Federal University of Technology, Minna, Niger State, Nigeria

***Corresponding Author**

DOI: https://doi.org/10.51584/IJRIAS.2025.10050007

Received: 26 April 2025; Accepted: 07 May 2025; Published: 28 May 2025

ABSTRACT

Two Electrical Geophysical methods were used at Biseni community in Bayelsa state to determine the effects of Oil spills on the subsurface resistivity in the area. Five Schlumberger Vertical Electrical Soundings (VES) with a maximum Current electrode spread of 300.00m were carried out outside the polluted area while 2D Wenner array of 100.00m coverage was used at the spill location. The interpretation was done using computer programmes, IP2win for VES data and RES2DINV software for 2D data. The resistivity curve types obtained are QKA (VES 1), QA (VES 2), HKA (VES 3) HA (VES 4), and AKA (VES 5), to reveal heterogeneity nature of the subsurface in the area. Six continuous layers were identified from the 2D true resistivity distribution inversion. The first two layers, from VES 1 to VES 5, at depth (0.3m – 3.4m) have resistivity values ranging between 4.46 Ωm and 468.1 Ωm. Correspondingly, at the polluted location, at depth (1.25m – 3.75m), the resistivities recorded are between 11 Ωm and 47.46 Ωm. The next two layers (three and four) situated at depth interval (1.7739 m – 69.85 m) have minimum and maximum resistivity values of 6.38 Ωm and 344 Ωm respectively. Res2inv imaging revealed resistivity between 2.52 Ωm and 11.6 Ωm situated at 3.75m to 8.44m depth. The last three layers (five, six and seven) outside the location have 3.29 Ωm to 31443 Ωm resistivity between 13m and 69m at the substratum. The 2D imaging have 0.133 Ωm to 2. 0 Ωm at depth interval 8.44m to 15.9 m. It shows lower resistivity values at the polluted site and this reduction (0.133 Ωm – 2.52 Ωm) continues downward into the substratum. However, outside the polluted site, the resistivity increases downward in VES 2, 3, VES 4 and VES 5, with recorded values of 31443, 8203, 2051 and 261 Ωm respectively, while high and low resistivity alternate in VES 1. The resistivity values encountered at the Oil spills side range between 0.031 - 900Ωm, and 45.32 to 9347 Ωm at the control location. The depth at about 16.00m, marked the limit of contamination, as indicated by observed reduced resistivity but increased in values beyond this point.

Keywords: IP2win, RES2DINV, Schlumberger, Resistivity. Wenner array.

INTRODUCTION

The release of Crude Oil into the Soil through Oil spills is receiving critical attention due to the potential risk posed to the ecosystem. Oil spillage may occur during transportation (both land and sea) and as leakages through storage tanks during drilling process. Irrespective of the sources of contamination, once it occurs it has negative effects on the environment [1]. Oil pollution represents a significant and persistent global environmental challenge, with a widespread and destructive impact on ecosystems. The contamination by Oil, even at relatively low levels, has a significant impact on the chemical, physical, biological and morphological properties of the soil. These changes disrupt the soil structure, hinder the activity of soil organisms and compromise plant health, ultimately affecting the broader ecosystem. [2]. The findings demonstrated that Oil contamination diminished the capacity of different soils to retain water, as capillary moisture capacity decline. The reduction in capacity is accompanied by an increase in hydrophobic processes, which render the soils

ISSN No. 2454-6194 | DOI: 10.51584/IJRIAS |Volume X Issue V May 2025

more resistant to water infiltration and retention [3]. There are two different types of contaminants: organic and inorganic. Hydrocarbons are organic compounds containing Carbon and Hydrogen in crude oil and natural gas but most contaminants comes from oil compounds [4].When it comes into contact with the soil, it alters, among other things, the physiochemical properties of the soil. The extent of variation depends on the soil type, the specific composition and quantity of the hydrocarbons. The wastes from the petroleum hydrocarbon discharged on the ground finally finds its ways to the soil system and change the properties of the soil like pore fluids, electrical resistivity, liquid limits, pH and unconfined compressive strength [5]. It is estimated that million tons of oil has been spilled in the Niger Delta ecosystem over the last 50years. Incidence of oil spill has become so rampant in the Oil producing region that made the British broadcasting corporation after visiting Bayelsa and Rivers state in May 2009 to describe Nigeria as "World Oil pollution capital" [6]. The major causes of oil spillage are corrosion of pipelines and tank accidents (50%), sabotage (28%), Oil production and operation (21%) and Engineering and drills (1%) [7].

Crude Oil still affects many countries because it is one of the essential fuel sources. Nevertheless, one cannot ignored the pollution caused by its use in industries such as mining, transportation, and Oil and gas business. As such Soil pollution is an issue in most communities because it influences people and ecology[8]. Tracing the subsurface oil leakage is essential to correctly plan the environmental preservation effects and reduce its hazards particularly on the groundwater. The electrical resistivity technique is considered a powerful tool for tracing the subsurface pollution in an acceptable manner. The crude oil shows a high resistivity signature, whereas the processed and degraded oil has a relatively low resistivity character [9]. At the initial stage, Oil contamination leads to an increase in the underground resistivity. However, overtime, Oil undergoes biodegradation as it moves downwards gradually and stops, there is a decrease in resistivity to reflect microbial activity and degradation. The observed change in resistivity is a key indicator used in geophysical investigations to assess the extent and depth of Oil contamination. This information has been used to the choice of method used in work The electrical resistivity of any material is the resistance between the opposite faces of a unit cube of the material. Resistivity is an internal parameter of the material through which current is compelled to flow and describes how easily this material can transmit an electrical current. In electrical resistivity surveys, a set of electrodes is placed at the surface of the ground, and an electrical current (D.C.) is injected into the subsurface. The resulting voltage difference is measured, and the apparent resistivity is calculated. By varying the electrode spacing and configuration, geophysicists can collect data at different depths, generating resistivity profiles that provide insights into subsurface structures. 2-D Wenner subsurface profile method or resistivity mapping is a method that aims to study the horizontal resistivity variation of the subsurface layers[10]. For Vertical electrical sounding, the Schlumberger array is preferred for deep penetration measurements due to its ability to detect variations in resistivity at greater depths compared to other electrical resistivity methods [11]

Description of study area

The study area is in Yenagoa local government area in Bayelsa state (Fig.1). This area lies along latitudes between 4^0 4' 00'' North and 5^0 24' 10'' North; and longitudes between 6^0 12' 00'' East and $6^0$39'30'' East and situated in the southern part of the Niger Delta of Nigeria. Geographically, Yenagoa is situated within the coastal area of the Niger Delta sedimentary basin. The ground surface is relatively flat and the sloping is gentle towards the Atlantic Ocean in the South with a mean elevation of about 10 m above mean sea level. It is drained by tributaries of River Num, Orashi River and Talyor Epie Creek with an average temperature and rainfall of 26.7 ^oC 2,899 mm respectively [12] The three major depositional typical of most deltaic environments, marine, mixed and continental are observable in the study area. These are represented environments by the three chrono-sratigrapic units namely, the Benin, Agbada and Akata Formations. Benin Formation can be described as a continental megafacies that overlies the Agbada formation. This formation comprises of late Eocene to recent deposits of alluvial and upper coastal plain deposits that are up to 2000m thick unconsolidated sands with thin clay and lignite interbeds [13] . It is said to be the major aquiferous formation within the Niger Delta region which consists of an inter-bedded sequence of sand and shales [14]. Agbada formation is mostly characterized by transgressive marine barrier foot deposits and tidal channel deposit and the covers the subsurface of the entire delta and has its lateral equivalence as poor sorting which probably indicates a fluvial origin The lithological composition of this formation comprises of sand stone

ISSN No. 2454-6194 | DOI: 10.51584/IJRIAS |Volume X Issue V May 2025

lenses at the top with a uniform grey sand silty shale at the base [15]. The Akata Formation, at the base of the Delta, is of marine origin and is composed of thick shale sequences (potential source rock), turbidite sand (potential reservoirs in deep water), and minor amount of clay and silt. Thin sandstone lenses occur near the top particularly near contact with the overlying Agbada Formation

METHODOLOGY

The Terrameter SAS 1000 resistivity equipment was used for both surveys which involved for 1-D, Schlumberger electrode array and for 2-D, Wenner array. SAS (Signal Averaging System) is a method whereby consecutive readings are taken automatically and the results are averaged continuously. Vertical electrical sounding (VES) using Schlumberger array electrode configurations was carried out by applying current into the ground through two current electrodes (A and B) and then measuring the resultant potential difference (V) between the potential electrodes (M and N). The center of the electrodes array remains fixed but the spacing's of the electrodes was increased so as to obtain information about the stratification of the ground [16]. The choice of electrode configuration was based on the requirement for vertical resolution [17].

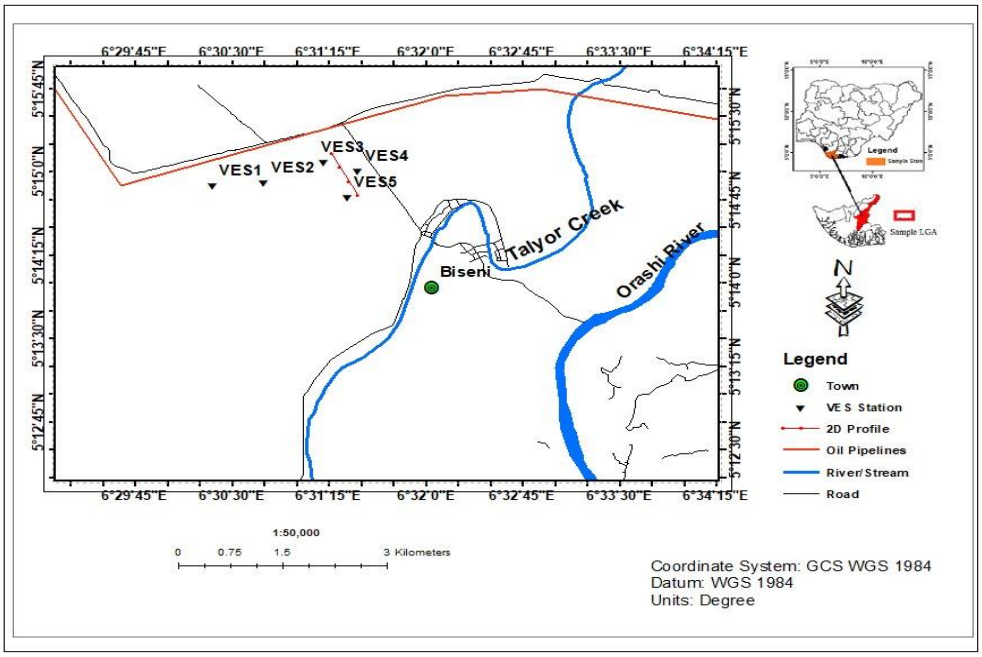

Fig. 1: Map of the study area showing the Vertical Electrical Sounding (VES) locations and 2-D profile.

In Schlumberger arrangement, (Fig.2), it is required that MN, the distance between potential electrodes must never exceed 2/5 of AB/2 where AB is the distance between current electrodes that is 5MN ≤ AB. [18] The field procedure consists of expanding AB while MN was fixed. The process yields a rapidly decreasing potential difference across MN which ultimately exceeds the measuring capabilities of the instrument and then a new value for MN was used. Thus field measurements were taken at AB/2 equals 1.00, 1.50, 2.00, 3.00, 5.00 6.00, 8.00, 10.00, ……150.00 m. The corresponding values of MN were 0.25, 0.5, 1.0, 2.5, …… 10.00 m. The depth of investigation is of the order of 0.1 to 0.3 times the AB length [19] . As such, the depth for which information is required determines the current electrode separation. Each time the current or potential or both electrodes were expanded, the value of the resistance R measured by the Terrameter was recorded. This was done for all the five stations. The value of the Geometric factor K each time the electrodes were expanded was calculated using the general equation for four electrodes spread, [4]

$$K = 2\pi\left[\frac{1}{r_1} - \frac{1}{r_2} - \frac{1}{r_3} + \frac{1}{r_4}\right]^{-1} \quad (1)$$

where $r_1 = C_1P_1$ (AM), $r_2 = P_1C_2$ (MB), $r_3 = C_1P_2$ (AN), $r_4 = C_2P_2$ (NB) from Fig.2.The product of the resistance R, read on the Terrameter and the geometric factor K (eq. 1) gives the apparent resistivity ρ_a.

ISSN No. 2454-6194 | DOI: 10.51584/IJRIAS |Volume X Issue V May 2025

$$\ell_\alpha = K\frac{\Delta V}{1} = KR \qquad (2)$$

Using IP2WIN computer software for the inversion, the apparent resistivity ρ_a was plotted against the half current electrodes (AB/2) spacing shown in Fig. 3 to Fig.7.

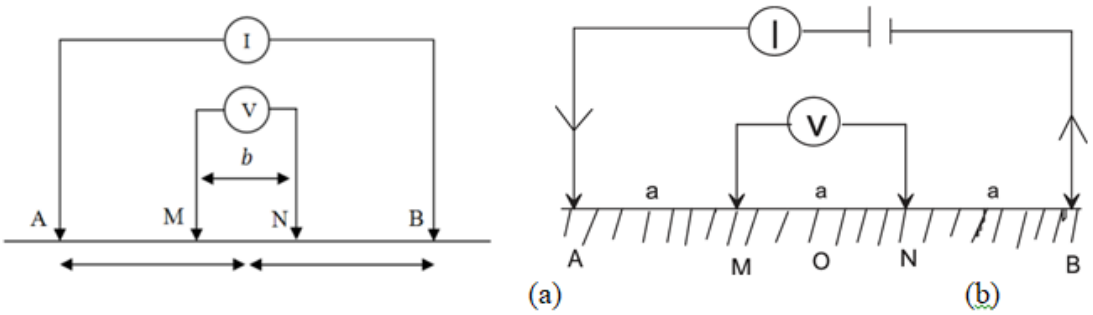

Fig.2: (a) Schlumberger array. And (b) Wenner array A and B are current electrodes while M and N are potential electrodes [20]

The 2-D imaging was carried out at the polluted location using Wenner spread on a profile line of 100.00m, Fig, 1. The procedure involved moving the whole system after each reading along the profile. The electrodes were uniformly spaced at 5.00m, 10.00m, 15.00m and 20.00m. After completing the sequence of measurements with 5.00m spacing for whole length of the profile, the next sequence of measurements with 10.00m was made and so on till the last electrode spacing.

From (eqn.1), by substituting a = AM= NB = r_1= r_4, r_2= r_3 = MB = AN = 2a, the Geometric factor $K = 2\pi a$
The Apparent resistivity, from equation (2), is therefore given as

$$\rho_\alpha = 2\pi\alpha\frac{\Delta V}{I} = 2\pi\alpha R, \qquad (3)$$

where R is the reading on the Terrameter. The 2-D resistivity inversion obtained, using RES2DINV software, is shown in Fig. 7.

RESULTS AND DISCUSSION

Table 1 represents the summary of the geoelectric layers and lithology obtained from for VES1-VES 5 which served as the controls site. The interpretations of the data, using IP2WIN software, of the five Vertical electrical soundings (VES), where readings were taken away (which served as the control site) from the 2-D profile located at the polluted site, are shown in Fig. 3 to 7. For each of the stations, geo-electrical layer, field and theoretical curve were obtained (Fig. 3-Fig.7) and the corresponding lithology presented in Fig. 8. The computer program, Res2Dinv resistivity inversion of acquired 2-D data is shown in Fig.9 that represents (a) apparent resistivity of field data (b) apparent resistivity of calculating data and (c) true resistivity distribution of inversion result. The acquired data profiles have been processed through the RES2DINV software utilizing the high damping factor and smoothness constraint ArcGIS 10.5 computer based software was also employed to map the subsurface resistivity of the layers for the VES stations occupied (Fig. 10 – 12).

For each of the inversion for the data, the root-mean-square errors are reasonable ranging between 0.256 - 0.978%; specifically 0.32%, 0.978%, 0.025%, 0.458% and 0.025% for VES1, VES 2, VES 3, VES 4 and VES 5 respectively. The resistivity curves obtained in the study area are four types: QKA for VES 1, QA for VES 2, HKA for VES 3, HA for VES 4 and AKA for VES 5. The resistivity curve obtained in this station, VES 1, was QKA (Fig. 3.). The unconsolidated loose topsoil has resistivity of 222.4 Ωm and about 0.3m depth from the surface. The next three layers of resistivities 4.46, 28.03 and 6.38 Ωm could be considered as wet Clay of various forms. The average resistivity being 12.7976 Ωm. These layers have a combined thickness of 5.584 Ωm. The next layer has the highest resistivity of the station, 1751 Ωm, and could be coarse Sand. The

ISSN No. 2454-6194 | DOI: 10.51584/IJRIAS |Volume X Issue V May 2025

substratum layer six from a depth 7.4m, which has a resistivity of 8.22 Ωm, is wet Clay.

Computer interpretation technique identified seven layers in VES 2 (Fig. 4), and gave a QA resistivity curve. The first two layers of resistivities 468.1 Ωm (topsoil) and 420.4 Ωm (fine Sand) with a combined thickness of 1.342m could be considered as topsoil of various compositions. The next three layers could be wet Clay of roughly different textures having resistivities of 47.79, 60.19 and 40.1 Ωm to give an average of 49.6 Ωm. The resistivity of this formation increase remarkably from layer five (40.1 Ωm), layer six (9347 Ωm) down to the substratum at a depth of 33.54m with a resistivity of 31443 Ωm. The last two layers six and seven could be considered as coarse Sand and coarse Sandstone respectively. VES 3, Fig. 5, gave a resistivity curve HQA of a six layer stratifications. The topsoil is underlain by lower resistivity in the next two layers (5.438 and 9.748 Ωm) with a total thickness of 2.7475m wet Clay. This could be a fine Clay deposit. Resistivity increases sharply in the next layer four to 73.54 Ωm at 3.3m depth with a thickness of 18.74m. The underneath layer harbours a lower resistivity of 36.07 Ωm and thickness 16.19m at 22.06m depth. The last layer, which could be sand, has a remarkable highest resistivity of the station, being 8203 Ωm from the depth of 38.25m to the subtratum.

Resistivity curve HA of five layers was revealed in VES 4 (Fig. 6). The topsoil of thickness 1.7m and resistivity of 11.12 Ωm is underlain by a lower resistivity of 7.462 Ωm having a thickness of about 1.5m. The third layer has a higher resistivity of 344 Ωm at about 3.2m depth but with a thickness of 12.53m. This third layer, medium fine Sand, lies on much lower resistive formation (63.25 Ωm) but of remarkable thickness (54.13m) more than all the layers above. This could be fine Clay. The last layer, which is coarse Sand, has a resistivity of 2051 Ωm is situated at about 70m to infinite. VES 5 is a six-layer stratification, Fig.7, that gives AKA-type resistivity curve. The first three layers, ,topsoil and Clay, with a combined depth of 3.0m, have resistivities of 10.96 Ωm, 26.18 Ωm and 14.39Ωm, at the surface, middle and base respectively. Layer four, which could be fine sand, 3.71m in thickness and 3m below the surface, has a resistivity of 220.5 Ωm. This overlies a much lower resistive wet Clay of resistivity 45.32 Ωm at 6.771m depth below the surface and 27.68m in thickness. The subtratum layer, which could be fine Sand 34.39m below the surface, has the highest resistivity of the station, being 261.3 Ωm in value. Here, resistivity increases downward. In all the stations, resistivity increases down to the substratum in VES2 – VES5 except VES 1. Figure 8 shows the Lithology for VES 1 – VES 5 up to a depth of 16m which is later compared to 2-D inversion in Fig.9c

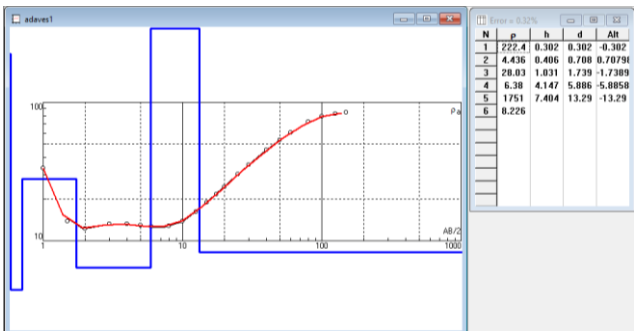

Fig. 3: Geoelectric Layers, Field and Theoretical Curve for VES 1

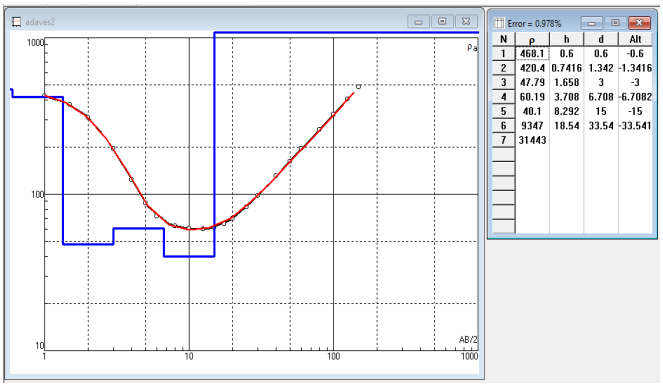

Fig. 4: Geoelectric Layers, Field and Theoretical Curves for VES 2

ISSN No. 2454-6194 | DOI: 10.51584/IJRIAS |Volume X Issue V May 2025

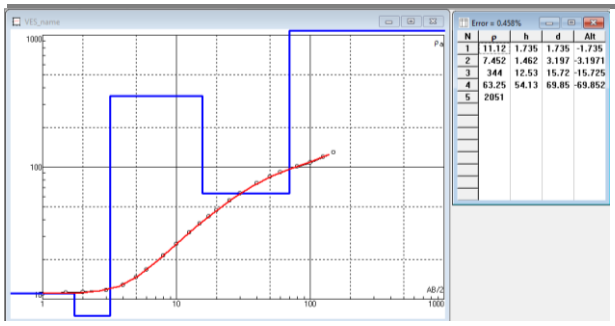

Fig. 5: Geoelectric Layers, Field and Theoretical curve for VES 4

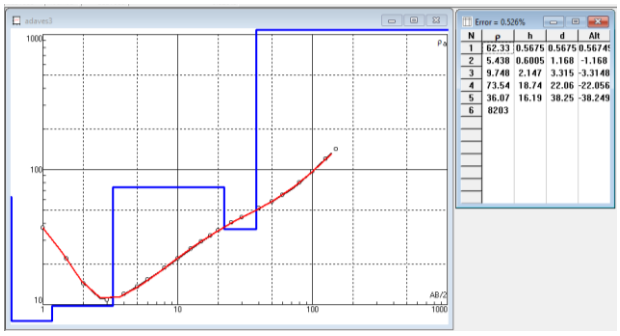

Fig.6: Geoelectric Layers, Field and Theoretical Curves for VES 3

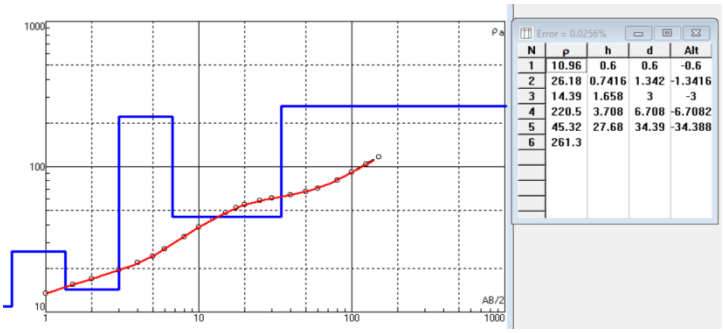

Fig. 7: Geoelectric Layers, Field and Theoretical Curves for VES 5

Table 1: Summary of the geoelectric layers and lithology for VES1 – VES 5

VES 1					VES 2			
Layer	Resistivity/Ωm	Thickness/m	Depth/m	Lithology	Resistivity/Ωm	Thickness/m	Depth/m	Lithology
1	222.4	0.302	0.302	Topsoil	468.1	0.6	0.6	Topsoil
2	2.236	0.406	0.708	wet Clay	420.4	0.7416	1.342	fine Sand
3	20.03	1.031	1.739	wet Clay	47.79	7.658	3	wet Clay
4	6.63	4.147	5.886	wet Clay	60.19	3.708	6.708	Clay
5	1751	7.404	13.29	Coarse sand	40.1	8.292	15	wet Clay
6	8.226			Wet Clay	9347	18.54	33.54	Coarse sand
7					31443			Coarse sand
VES 3					VES 4			
Layer	Resistivity/Ωm	Thickness/m	Depth/m	Lithology	Resistivity/Ωm	Thickness/m	Depth/m	Lithology
1	62.33	0.5675	0.5675	Topsoil	11.2	1.735	1.735	Topsoil
2	5.438	0.6005	1.168	wet Clay	7.452	1.462	1.735	wet Clay
3	9.748	2.147	3.315	wet Clay	344	12.53	15.72	medium fine Sand
4	73.54	18.74	22.06	Clay	63.25	54.13	69.85	Clay
5	36.07	16.19	38.25	wet Clay	2051			Coarse sand
6	8203			Coarse sand				
VES 5								
Layer	Resistivity/Ωm	Thickness/m	Depth/m	Lithology				
1	10.96	0.6	0.6	Topsoil				
2	26.18	0.7416	1.342	wet Clay				

ISSN No. 2454-6194 | DOI: 10.51584/IJRIAS |Volume X Issue V May 2025

3	14.39	1.658	3	wet Clay
4	220.5	3.708	6.708	medium fine Sand
5	45.32	27.68	34.39	wet Clay
6	261.3			medium fine Sand

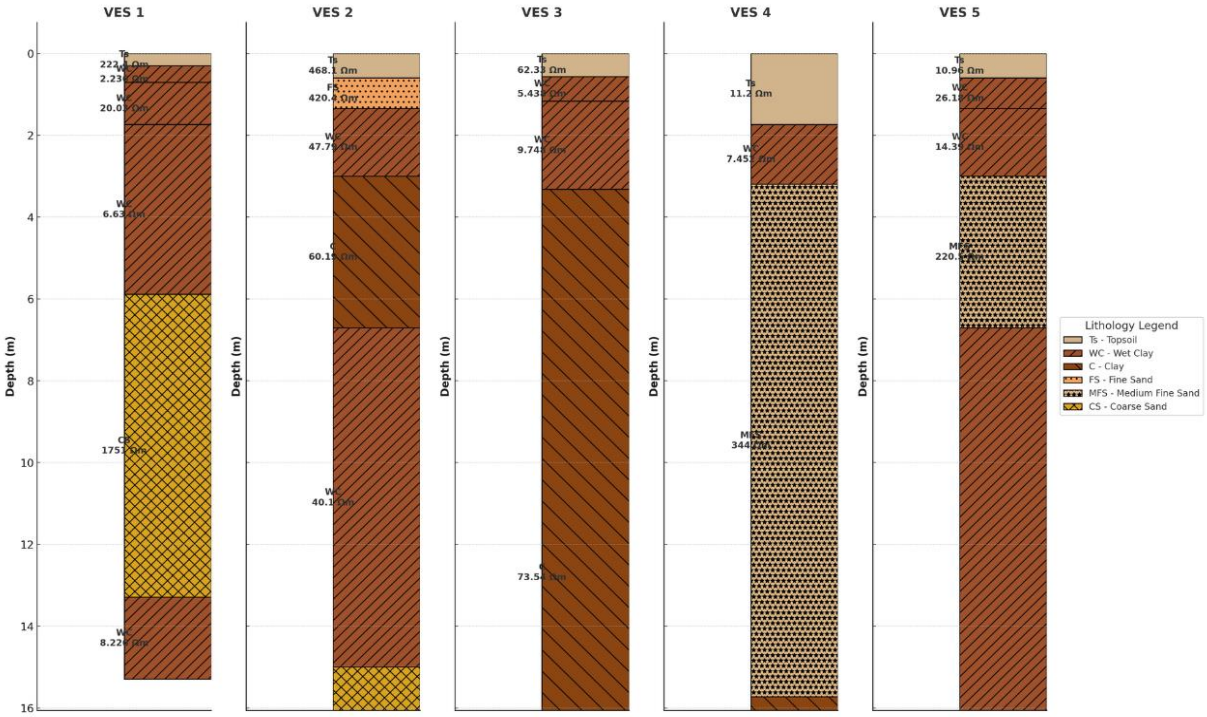

Fig. 8: Lithology for VES 1 – VES 5 for a depth of 16m.

From the results of 2-D resistivity inversion of data obtained at the polluted site, subsurface resistivity distribution was obtained, as represented by different colours in Fig.9.The first is the resistivity distribution based on measured Apparent resistivity of the field data, (Fig. 9a). The second is the resistivity distribution based on the calculated Apparent Resistivity (Fig. 9b).The image in (Fig. 9c) is the resistivity distribution of inversion results representing true resistivity obtained from the apparent resistivity and calculated data. From the inversion result, Fig. 9c, the range of resistivity obtained in the study area is between 0.031 - 900Ωm as indicated by various colours with a maximum depth of 15.9m.

Generally, three continuous layers and three that are not but of much lower resistivity and exist at the lower depth and continue downward beyond the depth of consideration (15. 90m), can be identified at this station. The first layer at the top with resistivity ranging from 11 to 47.6 Ωm is shown by different colours: Green, Yellow Green, Dark Green, Yellow, Slate Gray and Brown. It is situated between 1.25 and 3.75 m depth from the surface. This topsoil is made up of materials of different resistivities. The second layer has a resistivity range between (2.52- 11.5) Ωm. This traverses the whole length of the profile at depth 3.75 to about 8.44m below the surface. This is shown with three different colours: light Green, Slate Gray and Cyan. This layer consisting of various mixtures has most of the lower part (31- 40 m and 71- 100m along the profile) having the lowest resistivity between 0.5 and 2.0Ωm. The third layer has a resistivity range from 0.133 Ωm to about 2.0Ωm between the depth range of 8.44 m to 15.9m and beyond. Generally the resistivity decreases downward and along the profile (0 - 100)m. The distance along the profile (0 - 100) m, resistance represented in colours, and depth interval below the surface are indicated : (0-28)m, Slate Gray (2.0 Ωm) and depth (11.5-15.9)m ; (28-41.5)m, Cyan (0.50 Ωm) and depth (8.44-15.9)m; (1.5- 47.5m), light Blue (0.15 Ωm) and depth (8.44 - 11.95)m; (47.5 - 68)m, deep blue (0.133 Ωm) and depth (11.1- 15.9)m; (68 - 77)m, light Blue (0.15 Ωm) and depth (11.95 - 15.9m)m and the last portion (77 - 100)m, Cyan (0.50 Ωm), and depth (8.44 - 15.9)m. It is noted that the prevalent resistivity range here is between 0.133 - 47.6 Ωm existing at depth interval 1.25 - 15.9m.

ISSN No. 2454-6194 | DOI: 10.51584/IJRIAS |Volume X Issue V May 2025

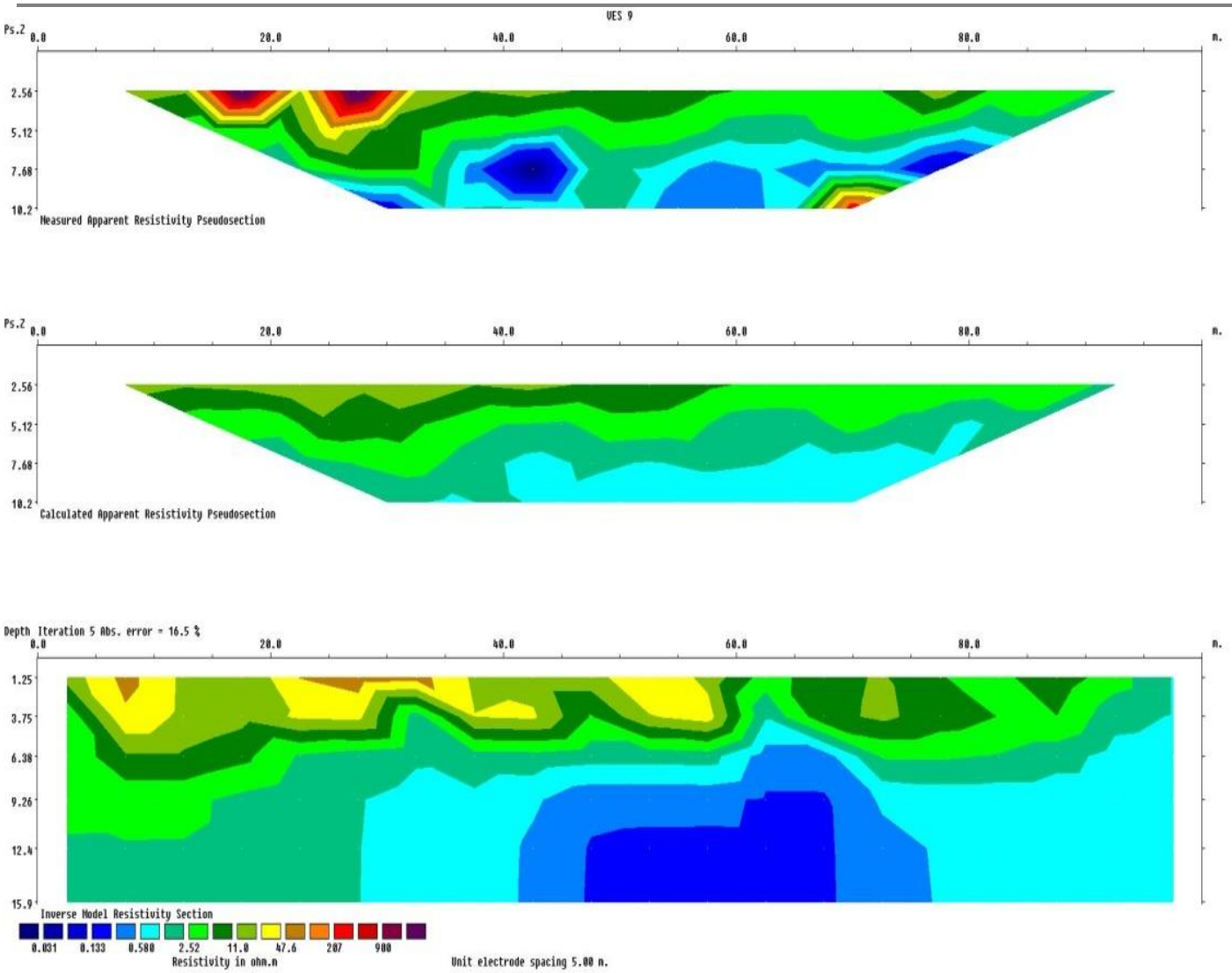

Fig.9: 2-D Resistivity inversion (a) apparent resistivity of field data (b) apparent resistivity of calculating data and (c) true resistivity distribution of inversion result

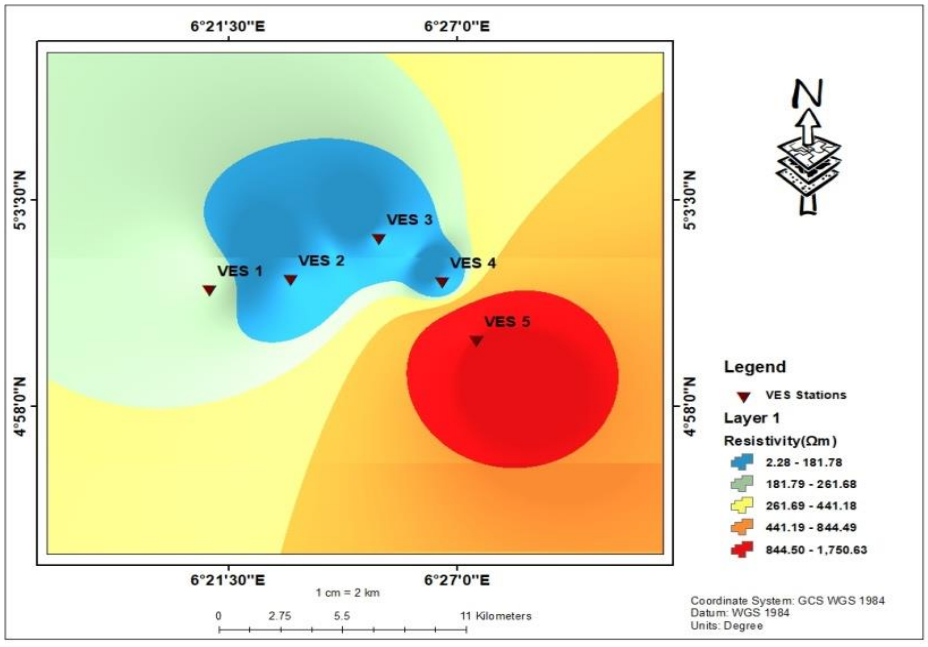

Fig.10: Subsurface resistivity cross layer 1 for the stations.

ISSN No. 2454-6194 | DOI: 10.51584/IJRIAS |Volume X Issue V May 2025

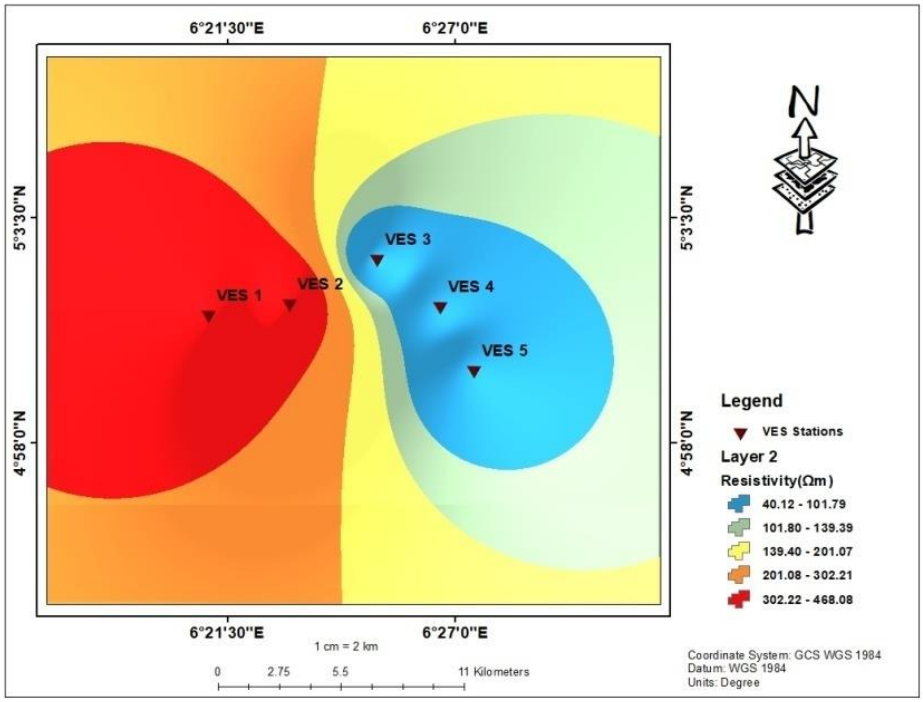

Fig. 11: Subsurface resistivity cross layer 2 for the stations

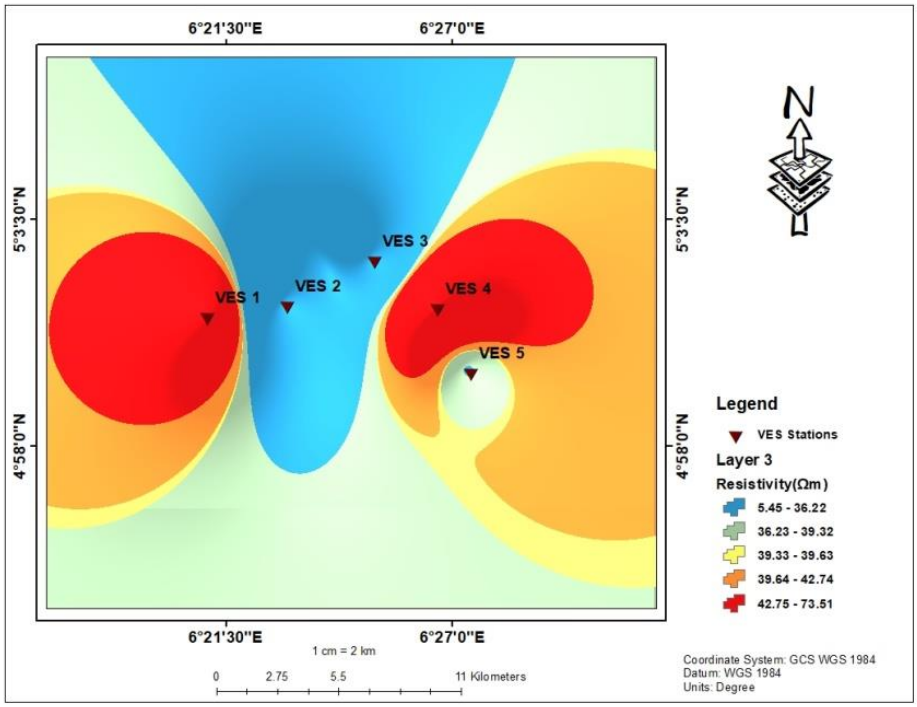

Fig.12: Subsurface resistivity cross layer 3 for the stations.

Comparison of results of 1-D imaging inversion and 2-D resistivity inversion

By considering the depth interval (1.25 – 3.75)m, the 2D inversion results (Fig. 9c) show resistivity ranging between 2.52 Ωm and 47.6Ωm. At the corresponding interval on VES 1 to VES 5 (Fig. 3 to Fig.7), the observed resistivity ranges from 11 Ωm to 468.1 Ωm. The layers that accommodate depths from 3.75m to 8.44m (Fig. 9c) have resistivity between 2.52 Ωm and 11.0 Ωm. From VES (1, 2, 3, 4 and 5), the resistivity value at this interval ranges from 40.1 Ωm in VES 2 to 1751 Ωm in VES 1 at (8 – 16)m below the surface of the contaminated location, remarkable low resistivity (0.133 – 2.0) Ωm was recorded and continues beyond the depth under consideration (Fig. 9c). Higher resistivity values (45.3 – 9347)Ωm were encountered at the corresponding depth at the VES stations. In all the stations away from the spills location, the resistivity

ISSN No. 2454-6194 | DOI: 10.51584/IJRIAS |Volume X Issue V May 2025

increases sharply downward to the last layer and beyond except VES 1 (Table 1). The percolation of crude Oil components has given rise to a much lower resistivity, up to a depth of about 16.00m considered, when compared to the surroundings soil's subsurface and at higher depth, resistivity increases downward. Using the ArcGIS software, three subsurface resistivity layers (Fig. 10, 11 and 12) were mapped across the VES 1 to VES5. The resistivities ranged between 2.28 – 844.54 Ωm for layer 1, 40.12 – 408.08 Ωm for layer 2 and 5.45 – 73.81 Ωm for layer 3. These layers correspond to the depths between 0.32 – 1.74 m, 0.71 – 1.74 m and 1.74 – 15.72m for layer 1, layer 2 and layer 3 respectively. The resistivity of the mapped layer 3 is significantly decreased at this depth (15.72 m) which is in agreement with very low resistivity, as a result of contamination from Oil spills, obtained from 1-D and 2-D analysis of Fig.3 - Fig. 7 and Fig.9 respectively.

CONCLUSIONS

This study reveals that Schlumberger vertical electrical sounding (VES) and 2D Wenner array are effective to study the effect of Oil spills on the subsurface resistivity of soil and can be applied to similar situation wherever. In general, the combination can be used to detect the changes in the underground resistivity/conductivity caused by any agent. Based on the interpretation of data collected, the following conclusion are drawn: The resistivity is lower at the polluted location than the surroundings within the study area . At the control side, the topsoil is mainly made up of dry sand and unconsolidated wet sand mixture of various textures, with resistivity values between 10.96 and 468.1 Ωm where the Vertical electrical soundings have been used. At the polluted site, the resistivity is very much lower to give reasons for the observed mixture of moist silt and Clayey sediment whose resistivity range between 11 to 47.6 Ωm in values. Each of the constituent layers tend to be of thicker dimensions as the depth below the surface increases for both polluted location and the control side within the study area. Resistivity varies horizontally and vertically at the polluted site where 2-D Wenner array measurement has been applied. However, where Vertical electrical sounding has been carried out, the trend of resistivity variation revealed was only vertical. The results from these observations and ArcGIS software mapping of the subsurface resistivity cross layers revealed that the contamination effect was prevalent at around 16.00m depth.

ACKNOWLEDGEMENT

This work has been made possible by the permission of Biseni community, on whose land the investigation was carried out. Therefore, I hereby express my profound gratitude to the leadership of this Oil producing community. It is pertinent to also express my appreciation to those who helped me in one way or the other during the laborious resistivity field work that produced these results. Finally, I thank Dr. Etteh, Desmond for the production of location map for this research at no cost.

REFERENCES

1. D.K. Talukka, and B.D. Saika. Effect of crude Oil on some consolidation properties of Clay soil. International Journal of Engineering Technology and advance engineering, 2013, vol.3 pp.117-120
2. R. Daryaee, A.A. Moosavi, R. Ghasemi, M. Riazi, Chapter 13 – Review of the Effects of Oil Pollutants on Physicochemical and Biological Soil Properties. In Biotechnology of Emerging Microbes; Sarma, H., Joshi, S.J., Eds.; Progress in Biochemistry and Biotechnology; Academic Press: Cambridge, MA, USA, 2024; pp. 263–297.
3. S. S. Oleg, S. G. Andrey, A. K. Valentina, Y. P. Yuliya, Y. B. Ruslan. E. Y. Aleksandr and A. S. Aleksandr, Effects of Oil Contamination on Range of Soil Types in Middle Taiga of Western Siberia. Institute of Nature and Technical Sciences, Surgut State University, Surgut 628412, Russia; Sustainability 2024, 16, 11204.
4. E. C. Shin, and B. M. Das, Bearing capacity of unsaturated oil-contaminated sand. International Journal of Offshore Polar Engineering. 2011, vol. 11, 3 , pp 220–226.
5. Pampanin, D.; Sydnes, M. Polycyclic aromatic hydrocarbons a constituent of petroleum: Presence and influence in the aquatic environment. Hydrocarbon 2013,vol 5, pp 83–118.
6. C. P., Nwilo, and T. O. Badejo, Laboratory studies on the influence of crude oil spillage on lateritic soil shear strength, a case study of Niger Delta area of Nigeria. Journal of Earth Science and Geotechnical

Engineering. 2009, 2(3), pp.73-83.
7. C.P., Nwilo, and T.O. Badejo. Management of oil spill dispersal along the Nigerian coastal areas. 2013 ISPRS Congress 2004, Istanbul, Turkey.
8. M. M. Haider, A. J. A. Yasir, A.A ., A. A. Ali A., S. R. Ali and B. M. Zaina, Effect of crude Oil on the Geotechnical properties of various soils and the developed remediation methods. Applied Sciences, 2023, 13, 1903
9. M. Mohamed, A. K. Mohamed, A. El-Said and E. Abeer, Tracing subsurface oil pollution leakage using 2D electrical resistivity tomography. Arabian Journal of Geosciences, 2013, vol 6, pp 3527 – 3533.
10. W. M., Telford, L. P. Geldart, and R.E. Sheriff,. Applied Geophysics. Cambridge University Press Cambridge, England, 1990, p.770.
11. M.H. Loke, Tutorial: 2D and 3D electrical imaging surveys. Available online from: www.geoelectrical.com. 2011).
12. O.A. Oki, and K.K., Oboshenure. Assessment of groundwater portability using quality Index approach in Tombia town Yenagoa, Nigeria. Journal of multidisciplinary Engineering science and Technology, 2017 vol. 4, 7
13. A. A. Avbovbo, Tertiary Lithostratigraphy of Niger Delta. Bulletin of American Association of Petroleum Geologist. 1978. vol. 62, pp. 297-306.
14. O. L. Asseez, ‘’Review of the Stratigraphy, sedimentation and structure of the Niger Delta’’ In: C. A. Kogbe, Geology of Nigeria, Rock View Nig Ltd., 1989, pp. 311-324.
15. I. S., Didei, and A Edirin,. Sedimentology of Stream sediments along the bed of Famgbe River in Yenagoa Area of Bayelsa State, Nigeria. Journal of Sedimentary Geology, 2018, vol. 4, pp. 1-18.
16. O.J. Akintorinwa, and O Abiola. Comparison of Schlumberger and modified Schlumberger arrays Vertical electrical sounding (VES) interpretation results. Research Journal in Engineering and Applied Sciences, 2012, vol.3, pp.190–196.
17. E. P., Soren, R. R., Keld, B. C., Niels, and C Steen. Evaluating the distribution of a shallow coastal aquifer by vertical multi-electrode profiling (Denmark). Hydrology Journal, 2010, vol. 18, pp.161-171.
18. J.E.A. Osemeikhian, and M.B. Asokhia. Applied Geophysics for Engineers and Geophysicist. Lagos: Samtos Services Ltd, Lagos. 1994
19. J. Bernard, ‘’Short note on the depth ofinvestigation of electrical methods’’. http://www.HeritageGeophysics.com 2003
20. D.S Parasnins. Principles of Applied Geophysics. (4thed.). London, Chapman and Hall, 1986